

https://dspace.org/

Trade with the West. Glass bowls of Eastern Mediterranean origin found in the courtyard of the Casas del Turuñuelo site (Guareña, Badajoz, Spain): archaeological context, analysis and conservation

González, Esther Rodríguez; Pérez, Sebastián Celestino; Medina Sánchez, María Cruz; Zucchiatti, Alessandro; Martín, Joaquín Barrio

2023-06
Elsevier
https://hdl.handle.net/10539/50251
Rodríguez González, E., Celestino Pérez, S., Medina Sánchez, M. C., Zucchiatti, A., & Barrio Martín, J. (2023, August). Trade with the West. Glass bowls of Eastern Mediterranean origin found in the courtyard of the Casas del Turuñuelo site (Guareña, Badajoz, Spain): Archaeological context, analysis and conservation. Journal of Archaeological Science: Reports. Elsevier BV. http://doi.org/10.1016/j.jasrep.2023.104029

Downloaded from a DSpace repository. https://dspace.org/

Journal of Archaeological Science: Reports 50 (2023) 104029



Contents lists available at ScienceDirect

Journal of Archaeological Science: Reports

journal homepage: www.elsevier.com/locate/jasrep





Trade with the West. Glass bowls of Eastern Mediterranean origin found in the courtyard of the Casas del Turuñuelo site (Guareña, Badajoz, Spain): Archaeological context, analysis and conservation

Esther Rodríguez González [a,*], Sebastián Celestino Pérez [a], María Cruz Medina Sánchez [b], Alessandro Zucchiatti [c,d], Joaquín Barrio Martín [b]

[a] Instituto de Arqueología (CSIC – Junta de Extremadura), Plaza de España, 15, 06800, Mérida, Badajoz, España
[b] SECYR – Universidad Autónoma de Madrid, Facultad de Filosofía y Letras, Módulo X, Planta Baja, Cantoblanco E-28049, Madrid, España
[c] School of Physics, University of the Witwatersrand, Private Bag 3, Wits 2050, South Africa
[d] DISTAV, Università di Genova, Corso Europa 26, 16132 Genova, Italy

ARTICLE INFO

Keywords:
Tartessos
Central Guadiana Valley
Glass bowls
Weathering
Conservation
PIXE
PIGE

ABSTRACT

The aim of this work is presenting a group of glasses excavated from the archaeological site Casas del Turuñuelo (Guareña, Badajoz, Spain), whose destruction dates back to the 5th Century BCE. Different types of glasses were found, among them two thick-walled translucent bowls and a very fine blue-coloured bowl. The study and conservation of these pieces has made it possible to characterize the composition of the different types of glass and their specific degradation, and to identify the possible origin where they were manufactured, in the Eastern Mediterranean. In addition, it has managed to recover the original surface and shape of these pieces and has given them the necessary consistency to be well preserved and studied.

1. Introduction

The site of Casas del Turuñuelo is an enclave located in the southwest of the Iberian Peninsula, specifically in the territory comprised by the Middle Guadiana Valley. This construction belongs to the category of settlement known as a Tartessian building hidden under a tumulus (Rodríguez González, 2018), constructions dated to the First Iron Age (6th-5th century BCE), of which a total of 14 examples are currently known (Fig. 1). Together with Casas del Turuñuelo, in the process of excavation, only two more buildings have been exhumed in their entirety: Cancho Roano (Zalamea de la Serena, Badajoz, Spain) and La Mata (Campanario, Badajoz, Spain), which provides us with excellent knowledge of constructions of this kind (Celestino Pérez and López Ruiz, 2016: 211-253).

Archaeological excavations at Casas del Turuñuelo began in 2014. Since then, four excavation campaigns have been carried out, which have documented the best-preserved earthen building in the Western Mediterranean (Celestino Pérez and Rodríguez González, 2020), as its two floors are still standing (Fig. 2a). So far, three rooms have been excavated from the upper floor: Room 100 (Rodríguez González and Celestino Pérez, 2017), a space measuring 70 m^2 to which a cultural functionality has been attributed due to the presence of an altar in the form of a bovid skin in its centre; room S-1 or the Banquet Room, from which a batch of materials was recovered linked with the celebration of a ritual banquet before the closure of the building (Rodríguez González and Celestino Pérez, 2019) and the north room, which is in the process of excavation, but where the only human remains documented to date at this site have been located.

Communication with the lower floor is via a monumental staircase almost 3 m high (Rodríguez González et al., 2020). This structure, located to the east, gives access to the courtyard, a space of 125 m^2 on the pavement of which a total of 52 animals were found to have been slaughtered, among which the remains of several horses stand out (Rodríguez González et al., 2020; Celestino Pérez and Rodríguez González, 2019) (Fig. 2b).

Unlike the other rooms excavated inside the Casas del Turuñuelo building, the objects recovered in the courtyard are not abundant, although they are exceptional. Two extremely rich assemblages from the

* Corresponding author.
E-mail addresses: esther.rodriguez@iam.csic.es (E. Rodríguez González), scelestino@iam.csic.es (S. Celestino Pérez), maricruz.medina@uam.es (M.C. Medina Sánchez), sandrozucchiatti@gmail.com (A. Zucchiatti), joaquin.barrio@uam.es (J. Barrio Martín).

https://doi.org/10.1016/j.jasrep.2023.104029
Received 13 October 2022; Received in revised form 20 April 2023; Accepted 25 April 2023
Available online 19 June 2023
2352-409X/© 2023 The Author(s). Published by Elsevier Ltd. This is an open access article under the CC BY-NC-ND license (http://creativecommons.org/licenses/by-nc-nd/4.0/).

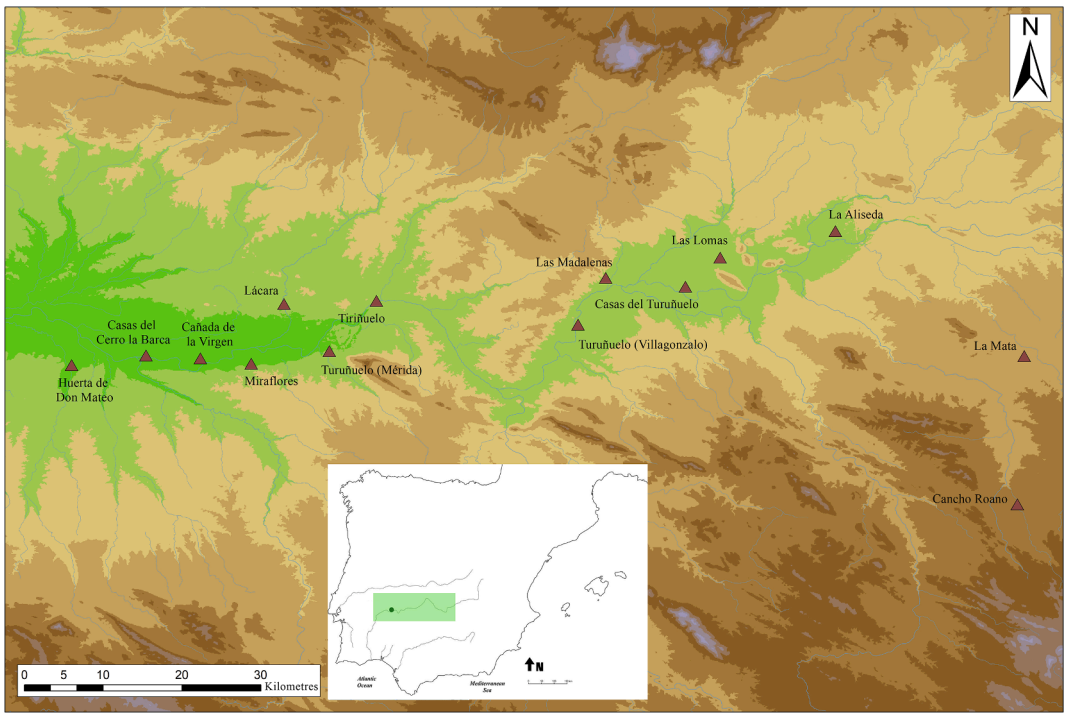


Fig. 1. Location map of the Tartessian buildings hidden under tumuli.

courtyard are unique examples of Iron Age archaeology in the Western Mediterranean. The first group was recovered from the space between the staircase and the northern boundary of the courtyard; it is a deposit from which a set of three Phoenician-Punic glass ointment jars, and a weighing system of seven bronze weights were recovered (Celestino Pérez and Rodríguez González, 2019: 352-353) and the oldest fragment of wool found so far in the Iberian Peninsula (Marín et al., 2019: 949); exceptional pieces to which are added the remains of two of the sacrificed equids, a sack amphora, a Greek imitation cup for wine consumption and several small burlap sacks containing barley seeds, among other objects. (Fig. 3).

The second group was found in front of the staircase. In the stratigraphic unit that covers the animal sacrifice, the remains of a marble sculpture were recovered, specifically the pedestal and the feet up to the start of the ankles, made of Pentelic marble (Athens, Greece) and polychrome, as remains of the blue and red paint used to decorate it are still preserved; together with the fragments of at least four glass bowls, whose conservation, analysis and historical reading are the subject of research in the present work (Fig. 4). Both the sculpture and the set of glasses constitute the earliest evidence of the presence of this type of imported material at a site on the Iberian Peninsula, hence the importance and uniqueness of this finding.

2. Objectives and method:

In order to study the glass bowls from the courtyard of the Casas del Turuñuelo site, we designed an interdisciplinary working protocol. The aim of this protocol is to achieve the following complementary objectives:

1. To evaluate the state of conservation of the fragments. To take care of the degradation processes in view of the objects restoration.
2. Recovering their shape and stability with the conservation treatment, so they can be correctly studied and contemplated without risk.
3. To perform instrumental analyses of a set of the recovered fragments to know better the glass technology at Tartessian period, and establish parallels with similar pieces known in the Mediterranean basin, with comparable typologies and composition.
4. Attempting to identify the origin of the materials with which the objects were made by typological comparison and isotopic analysis.

3. Materials and state of conservation[1]

The objects of this study were excavated during the 2017 campaign in the courtyard of the building, in a clayey stratum with ashes and charcoal, above the level of an animal sacrifice (Celestino Pérez and Rodríguez González, 2019: 354-355). All of them appeared very fragmented and covered with earth. Two thick-walled translucent bowls (SECYR 828 and 829), and a thin blue-colored bowl (SECYR 830, 831 and 833). Other groups of fragments (SECYR 831, 832 and 834) arrived in such a broken and fragile condition due to a severe weathering process that their conservation has not been possible. Many of these fragments were used to examine the corrosion state and analyse the composition.

3.1. Conservation of two translucent bowls

Two unique pieces for the context we are studying. The glass fragments identified as SECYR 828 and 829 formed two bowls, both incomplete, with similar external appearance and decoration, differentiated from each other by their shape and (see below) by the material (Fig. 5).

[1] Both the conservation of the pieces and their analysis have been carried out by the Conservation, Restoration and Scientific Studies of Archaeological Heritage Service (SECYR) of the Universidad Autónoma de Madrid. Its members are part of the team of the research project 'Construyendo Tarteso 2.0', directed by the Institute of Archaeology (CSIC - Junta de Extremadura), which includes the excavations at the site of Casas del Turuñuelo. SECYR is responsible for the conservation and analysis of the metal and glass objects from this site.



Fig. 2. A. Aerial view of the site of Casas del Turuñuelo (Guareña, Badajoz, Spain) (photograph from 2018). B. Photogrammetric view of the courtyard of Casas del Turuñuelo (Guareña, Badajoz, Spain).



Fig. 3. Photograph of the northwest corner of the courtyard of Casas del Turuñuelo (Guareña, Badajoz, Spain) with the deposit space for the materials indicated. A. Photograph of the bronze weight system. B. Photograph of the three vitreous paste ointment jars.

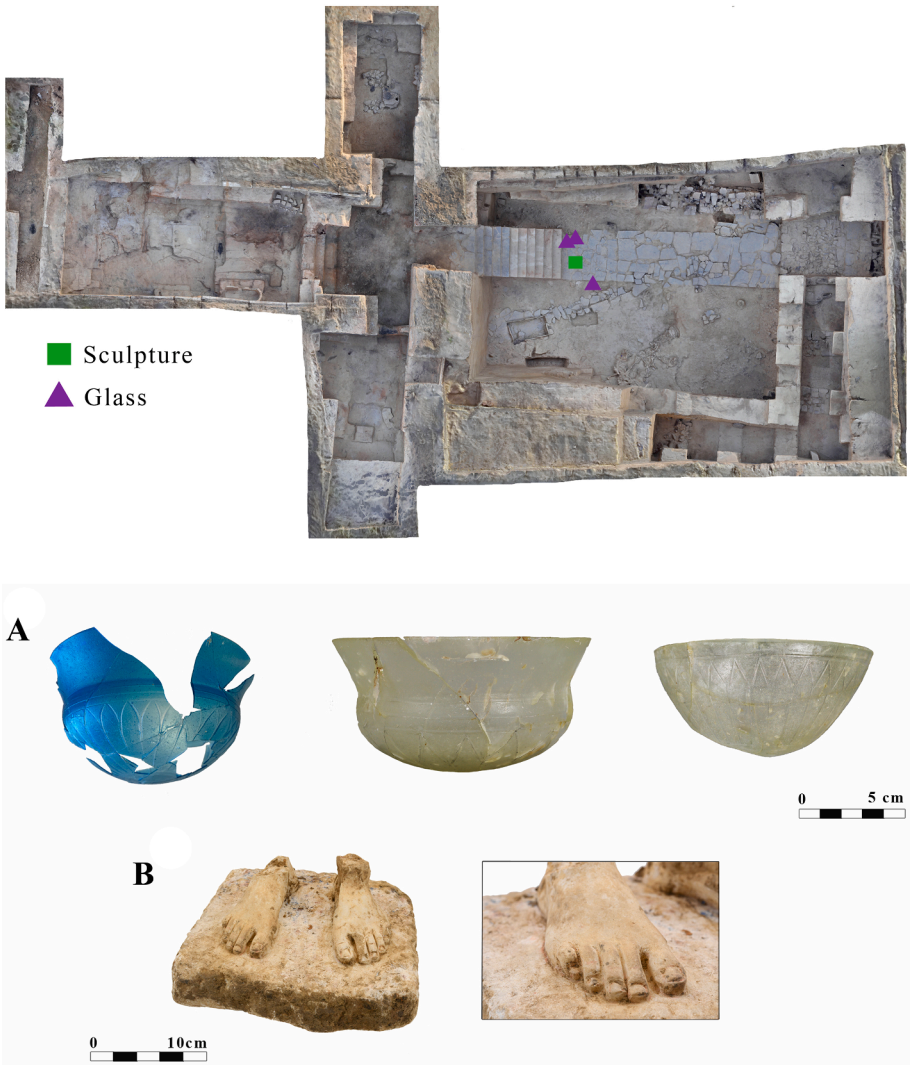


Fig. 4. Overhead view of the site of Casas del Turuñuelo (Guareña, Badajoz, Spain) showing the location of the glass bowls and the marble sculpture. A. Photograph of the three glass bowls studied Thin blue-coloured bowl, bell-shaped translucent bowl and translucent bowl. B. General and close-up photograph of the Pentelic marble sculpture (Athens, Greece).

The glass is slightly yellow, translucent and forms thick walls (between 3 and 4 mm after cleaning) which are decorated on the outer surface with an incised petal design with pointed ends. The glass thickness and its shape suggest a moulding technique (Goldstein, 1979:33; Ignatiadou, 2011; Schmidt, 2019), and the decoration was performed after cooling.

The biggest piece, SECYR 828, is characterized by having a large and wide neck that gives the bowl a flared shape. The decoration covers only the body, leaving the neck even. Petals start at the base and surround the contour only reaching the lower curve of the bowl. Above them, three parallel bands decorate the medium and wider part.

The glass is in general well conserved, it is stable despite the weathering of the first layers that caused iridescence on the surface and small cracks across the walls (Fig. 6). However, some small fragments were more affected by corrosion, as we could verify under optical microscopy and SEM (Fig. 7). The bowl is practically whole except for three small gaps that do not affect the stability or the sense of the piece.

The second bowl, SECYR 829, has a simple semi-circular shape. It is also decorated with a pattern of incised pointy petals, but in this case they are narrower, closer together and cover the whole surface reaching the mouth of the bowl, bordered with a band. The glass state of conservation, as in the previous case, is very stable. However, only about half of this bowl has been preserved, the rest is lost. It is surprising that the other fragments were not recovered, taking into account the excellent condition of those preserved and the clean fracture lines.

Their characteristics were observed and defined only after the cleaning process, once the external crust made of earthy deposits and the weathering was removed. At first sight these layers have a fine, whitish and opaque aspect. However, under optical microscope and SEM the glass transformation and the degree of decomposition was clearly identified. Far from being uniform, the crust is a succession of numerous layers that have lost their compactness, hence their extreme fragility and the ease with which they are removed. Weathering is the usual degradation of glass found in an archaeological context and is produced by contact with moisture, which dissolves the alkaline component of the outermost layers, causing the glass to lose compactness (Newton and Davidson, 1989).

3.2. *Conservation of the blue bowl*

The fragments corresponding to SECYR 830, 831, 833[2] were part of a blue glass bowl. It is a totally different glass from the rest of this study,

[2] We have received fragments of this blue glass gradually as they were found in different archaeological campaigns.



Fig. 5. Top SECYR 828, bottom SECYR 829 Initial state of conservation.



Fig. 6. Fragment of bowl SECYR 828 once the weathering crust was removed. The surface is very clean, and only small holes and fissures are visible. With time and bad environmental conditions, these could have developed in real cracks and fragments.

due to its intense blue colour and its thinness, which makes it look like blown glass, although this technology starts only in Roman times, during the First Century B.C. (Vigil Pascual, 1969:81). As in the case of the translucent bowls, the fragments were found covered with soil deposits and weathering, (Fig. 8). But unlike them, the deeper impact of weathering on these thinner walls has increased their weakness and provoked even more shattering in the small pieces. This was documented under optical microscope and SEM and the images obtained with both techniques revealed a significant loss of material, where the thickness of the wall with the laminated crust was twice the thickness of the cleaned core (Fig. 9, BSE image on the right). Moreover, the structure is absolutely filled with bubbles decreasing its consistency, which can be documented under magnifying glasses (Fig. 10). This complex state of conservation has made the fragments integration very difficult and although the shape, the perimeter and the decoration were recovered in the end, the resulting structure is still fragile (Fig. 11).

3.3. Conservation of the shattered glass

The glass objects previously described were relatively well preserved: a sufficient number of fragments were conserved to identify the shape of the object. As for their inner structure, with the exception of the weak blue glass that needed more time and care to be treated, glass was slightly affected by weathering but the core was stable, and fragments could be manipulated and cleaned without the risk of losing them. In

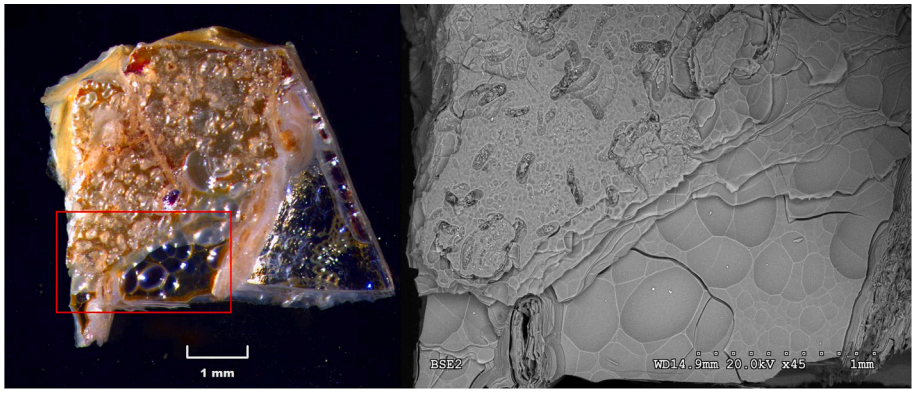


Fig. 7. Glass fragment from the bowl SECYR 828 that has been partially cleaned. Left: Optical photomicrograph where the area analysed with SEM-EDX is marked in red. Right: SEM BSE image where the succession of layers of the weathering crust can be distinguished.

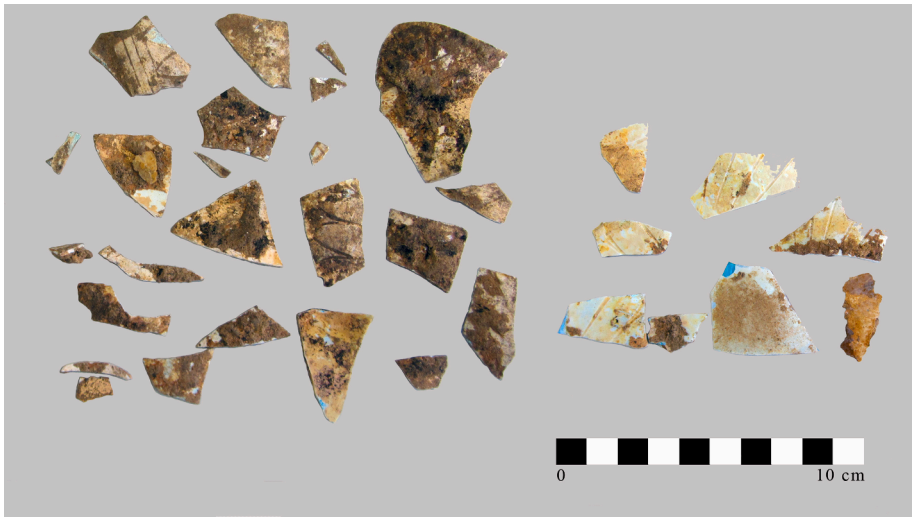


Fig. 8. Blue glass fragments. Initial state.

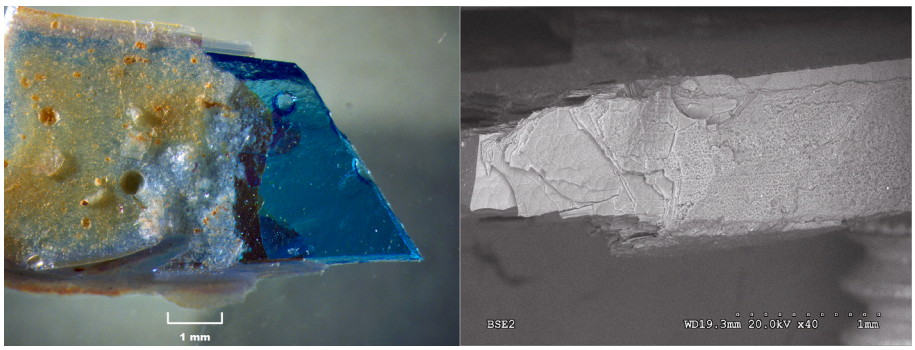


Fig. 9. Left: Photomicrograph of the blue bowl fragment half cleaned. Right: BSE image showing the thickness of the weathering crust formed by numerous layers.

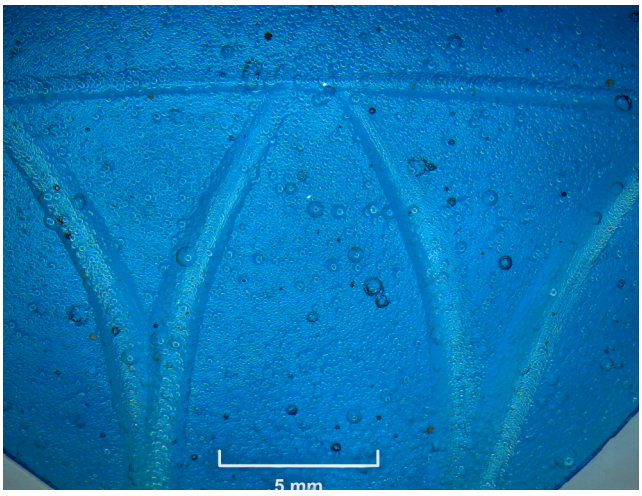


Fig. 10. Photomicrograph of the decoration of SECYR 833, where we can distinguish bubbles in all layers of the glass structure, both on the surface and inside.

contrast, the current groups of fragments were practically disintegrated (SECYR 832 y 834, Fig. 12). From the glass colour and the incised decoration, we can deduce that these fragments were part of a bowl similar to SECYR 828 and 829.

In SECYR 834 only six fragments had a minimum size to receive a conservation treatment, the rest were in such an unstable state of conservation that cleaning was useless, because the layers of corrosion encompassed practically the entire fragment, as showed the examination with optical microscopy (Fig. 13) and SEM-EDX (Fig. 14). This delicate structure lead to the collapse of the fragment when we carried out a cleaning test. The remaining piece had lost so much surface that it did not conserve its original shape and it was impossible to integrate the pieces together. What is the reason for this deeper deterioration state? Why the difference in conservation?

We have tried to find the answer to these questions, analysing the different factors that may have influenced their conservation: the materials, the manufacturing process, the useful life of the glass objects, how they were left behind, the burial conditions and, finally, the excavation process. Certain aspects remain unclear and will probably stay this way. For example, it is very unlikely that we will get information about the useful life of these vessels, given that their state of conservation makes it impossible to take samples of the content. Nevertheless, we have confirmed that the studied glass objects share most of these factors.

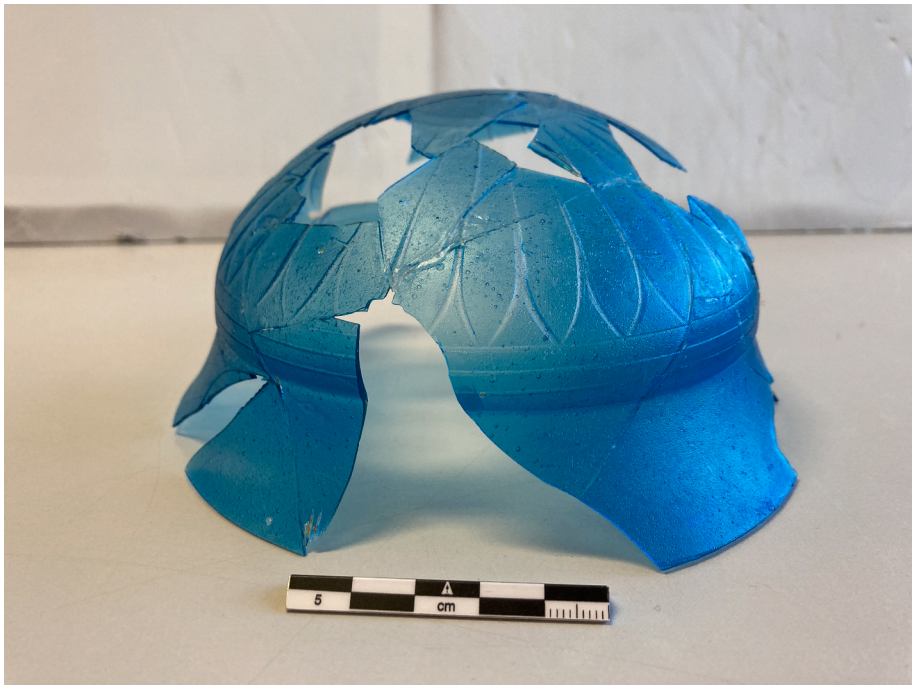


Fig. 11. Blue bowl final state.

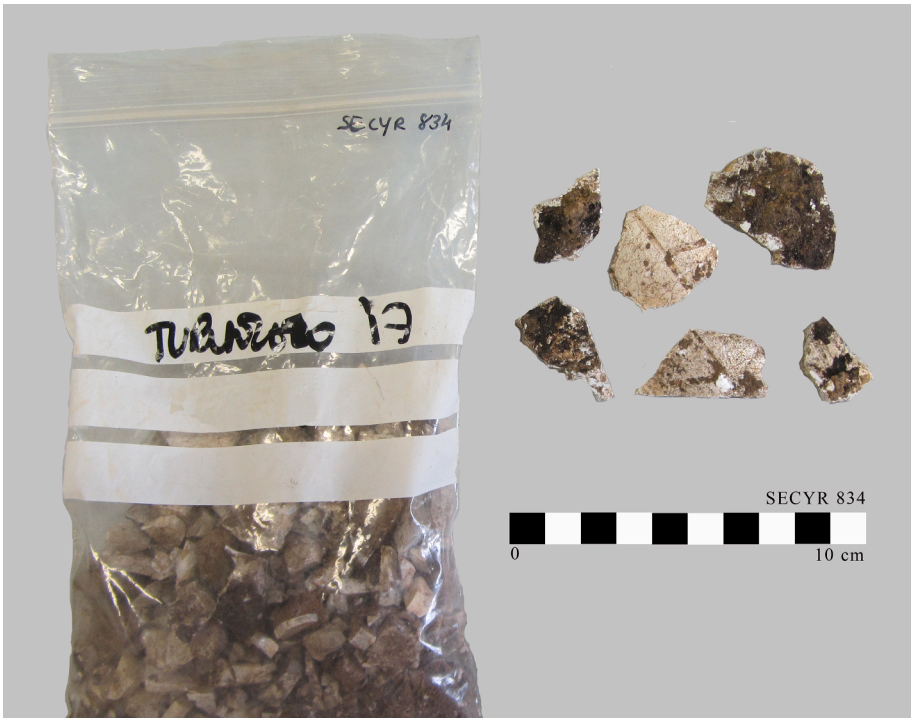


Fig. 12. SECYR 834. Initial state of conservation.

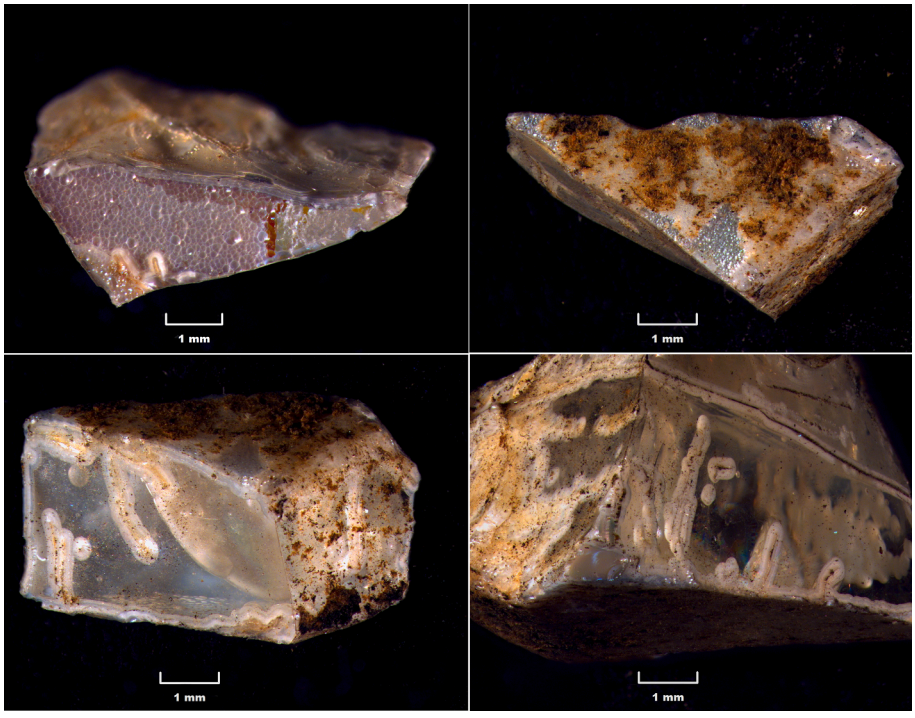


Fig. 13. Four views of a fragment of SECYR 834. The external surfaces show soil deposits and weathering, the inner areas show corrosion that extends through the walls and can continue to damage the piece. Top left image corresponds to the view analysed in SEM (Fig. 14).

Beginning with their chemical composition, analyses do not show important differences that explain such a diverse conservation[3]. Second, the possibility of an irregularity during the manufacture has been dismissed because it would have meant the vessels loss during the transport from the Eastern Mediterranean to the Iberian Peninsula (Palomar et al. 2022:160). Third, the burial conditions were the same for all these glass objects: they were found in the courtyard, close to each other and in the same archaeological layer of fire, surrounded by wet soil. In short, a very aggressive atmosphere for glass conservation; but this situation is common to all the pieces and it does not explain why pieces from SECYR

[3] Comparing the results in Table 2 for SECYR 828, SECYR 829 and SECYR 834, we find slight differences, which may derive from the fact that we have used punctual analytical techniques on samples with a very irregular state of conservation, and being SECYR 834 much more devitrified than the other two.

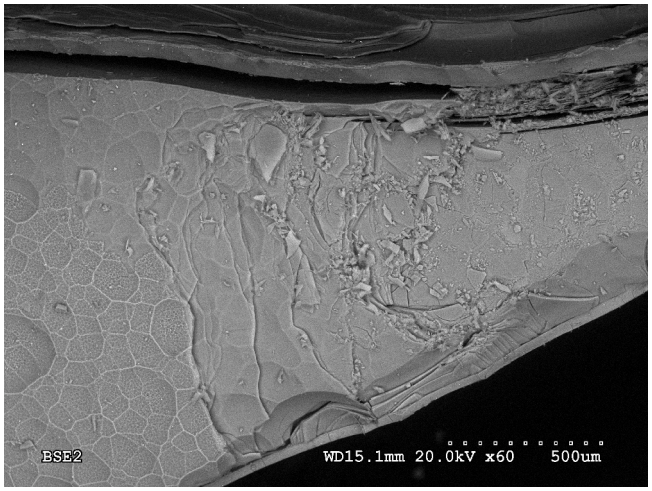


Fig. 14. Glass fragment SECYR 834 SEM-BSE image. On the left side of the sample the weathering crust is complete and has a cracked surface, and has been removed towards the right side. In the upper area, the crust is separated.

834 were much more destroyed than SECYR 828 and 829 (moreover, rests of ashes were found covering the fragments from these vessels, see Fig. 5). Fourth, the excavation process did not affect the glass shattering of SECYR 834 because it was found in this state.

Therefore, our proposal is to focus on the last determining issue: the deliberate and random destruction of these glass vessels during the building's wrecking and abandonment. There are numerous examples of intentionally destroyed objects at Casas del Turuñuelo. An example of this is the stone bathtub documented in Room 100 of the building (Rodríguez González y Celestino Pérez, 2017: 185). While the base of the container was located in its original place, the fragments that make up the rest of the piece have been recovered during the excavation work. Many of them were recovered in the yard fill. This evidence makes it possible to certify that the residents of the building, before its burning and destruction, broke many of the objects and threw the fragments at various points in the building.

4. Instrumental analysis of glasses

Some of the glass samples could be analysed at the facilities of the Universidad Autónoma de Madrid (SECYR, CMAM, SIDI) for elemental content and two at the CAI de Geocronología y Geoquímica Isotópica of the Universidad Complutense of Madrid for Sr-Nd isotope characterization.

4.1. Elemental analysis

Particle Induced X-ray Emission (PIXE) and Particle Induced

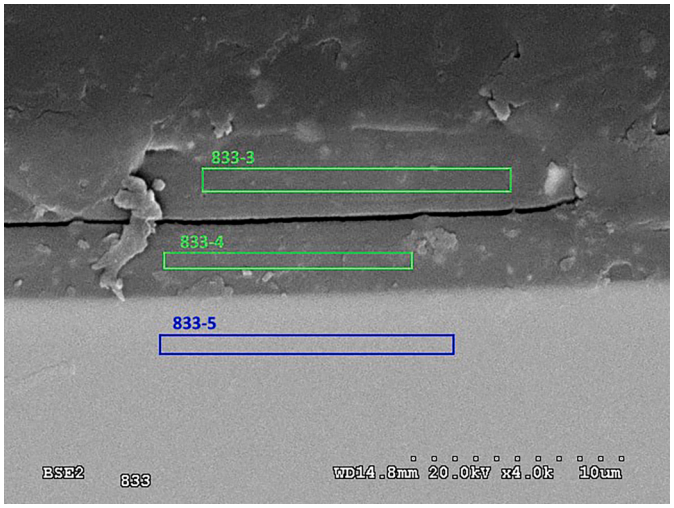


Fig. 16. A Scanning Electron Microscopy image of a cross section of sample SECYR 833 showing the areas where sodium concentrations was measured. Points 833–3 and 833–4 are in the devitrified layer, point 833–5 is in the glass bulk.

Gamma-ray Emission (PIGE) were simultaneously used at the Centro de Micro Análisis de Materiales (CMAM) to determine the elemental composition of the samples. PIXE and PIGE are intrinsically non-destructive. The samples were analyzed as received after the restoration done in the SECYR laboratory as explained above. Therefore, the loss of elements due to contamination and weathering cannot be excluded.

The PIXE analysis, performed with 3 MeV accelerated protons explores a sample depth of about 80 μm in an alkaline glass matrix and detects major (Na, Si, Ca), minor (Mg, Al, S, K) and trace elements (P, Cl, Ti, Mn, Fe, Co, Cu, Sr, Zr, Cd, Sn, Sb and Pb). A sensible comparison of compositions clearly requires the analysis of the glass bulk. Sodium, due to the low energy (1.041 keV) of its characteristic X-ray line and consequently its high attenuation coefficient, is detectable essentially in the first few microns (PIXE limit) of a sample, compared to the about 80 μm of the proton range. It is known that sodium has tendency to be removed from the glass matrix by ion exchange with the environment (e.g. Climent-Font et al., 2008). If a degraded surface layer extends above the PIXE limit, sodium in the bulk can only be quantified by PIGE, provided the degradation does not extend too much along the penetration depth of protons.

PIXE spectra were processed with the GUPIX package with the assumption that targets were thick and homogeneous and all elements were in oxide form. Combination of results from the two X-ray detectors of our system was done with a procedure explained elsewhere, checked by the use of standards (Zucchiatti et al., 2018).

Sodium concentration was determined measuring the yields of the

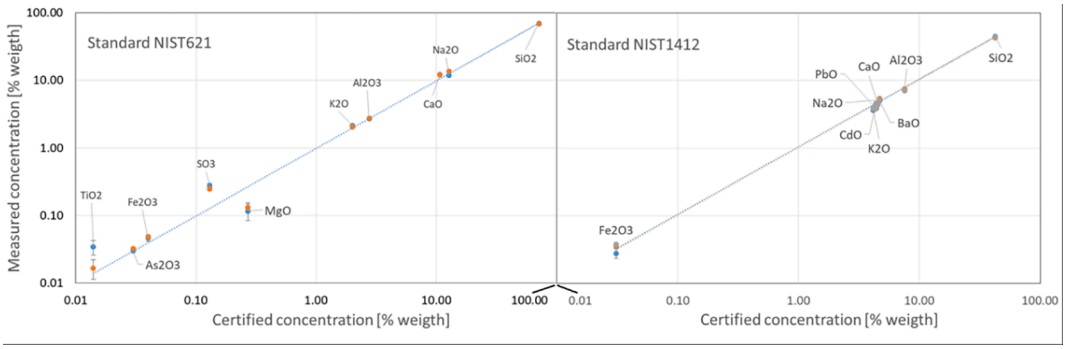


Fig. 15. Comparison with certified data of concentrations given by a combined PIXE-PIGE analysis on standards NIST 621 and NIST 1412.

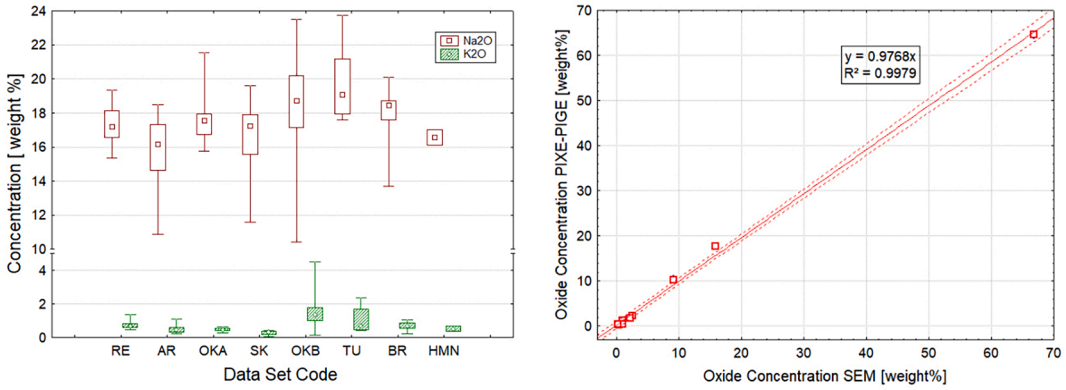


Fig. 17. (left) Na and K oxide concentrations of the Turuñuelo glasses compared to other sets of antique natron glasses. See below for codes. (right) The SEM oxide concentrations measured in the bulk of sample SECYR 833 compared to the ones extracted by the PIXE-PIGE method in the same sample.

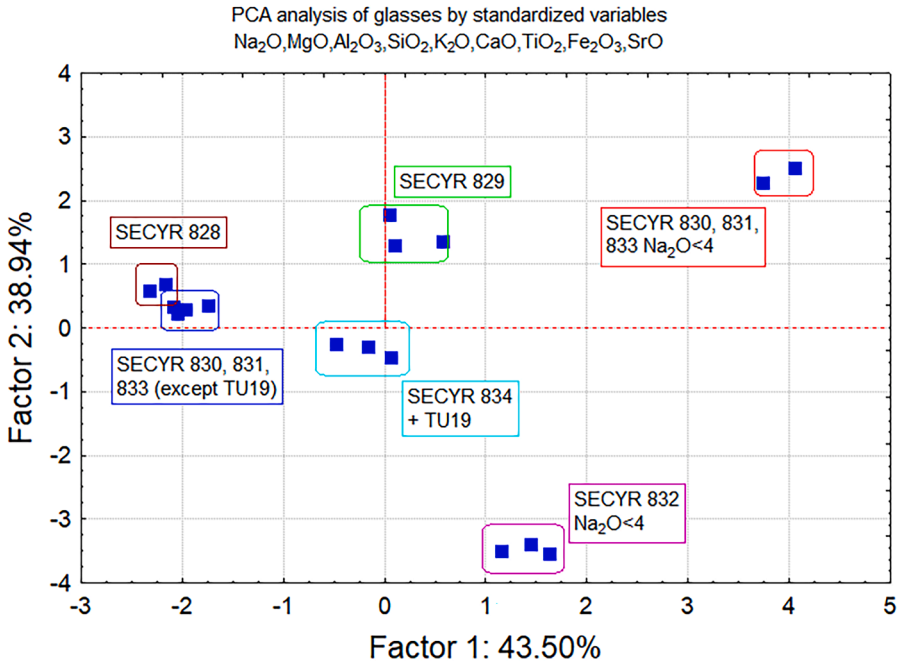


Fig. 18. Plot of the first two factors of a Principal Component Analysis of the Turuñuelo glass set performed using standardized concentrations of major and minor elements indicated in the plot.

Table 1
List of materials under study. It indicates the type of glass, its dimensions [4] and the inventory number given in the laboratory.

Object	Glass	Measurements in cm	Lab SECYR no.
Bell shaped bowl	Thick and translucent	Height: 7.2 Max. Diameter: 13.0 Glass Thickness: 0.3	828
Bowl	Thick and translucent	Height: 5.4 Max. Diameter: 12.7 Glass Thickness: 0.4	829
Thin blue-coloured bowl	Very thin and blue	Height: 7.6 Max. Diameter: 14.7 Glass Thickness: 0.1–0.3	830, 831, 833
Thick blue glass fragments	Thick and blue	The fragments are in such a poor state of conservation that their measurements are not representative.	832,834

[4] Glass thickness has been measured after cleaning. It is important to take this into account because the surface is partially lost due to the weathering process. However, one must take care of the fact that the cleaning might not have removed the whole corrosion layer as it has been demonstrated by a few microscopic analyses.

Table 2
Elemental concentrations expressed in weight percent of the oxide with the absolute error. Concentrations sum at 100%. Side = measurement taken on the fragment section. Surf = measurement taken on the fragment surf.

Object	Sample	Code	Na_2O		MgO		Al_2O_3		SiO_2		SO_3		Cl		K_2O		CaO		TiO_2	
Bell-shaped translucent thick bowl	828 side pt1	TU29	23.71	1.21	0.19	0.03	2.31	0.04	60.83	0.18	0.23	0.02	1.24	0.01	0.64	0.01	7.51	0.03	0.09	0.01
	828 side pt2	TU30	20.57	1.05	0.19	0.02	2.16	0.03	63.39	0.16	0.23	0.02	1.31	0.01	0.62	0.01	8.37	0.03	0.10	0.01
Translucent thick bowl	829 side pt1	TU26	23.64	1.21	0.31	0.03	6.13	0.05	59.38	0.16	0.23	0.02	0.52	0.01	2.35	0.01	5.24	0.02	0.06	0.01
	829 side pt2	TU27	20.81	1.06	0.36	0.03	6.15	0.05	61.01	0.15	0.25	0.01	0.62	0.01	2.36	0.01	5.61	0.02	0.08	0.01
	829 surf pt3	TU28	21.56	1.10	0.37	0.03	6.45	0.07	60.80	0.18	0.25	0.02	0.52	0.01	2.35	0.02	5.18	0.03	0.07	0.01
Thin blue-colored bowl	830 surf pt1	TU13	17.97	0.92	0.25	0.04	2.27	0.05	64.54	0.21	0.44	0.03	1.17	0.02	0.49	0.01	9.78	0.04	0.07	0.01
	830 surf pt2	TU14	17.93	0.91	0.27	0.02	2.31	0.04	64.26	0.16	0.46	0.02	1.18	0.01	0.46	0.01	9.91	0.03	0.07	0.01
	831 surf pt1	TU17	3.12	0.16	0.41	0.04	8.97	0.09	78.97	0.23	0.11	0.02	0.05	0.01	5.81	0.03	1.43	0.02	0.03	0.01
	831 surf pt2	TU18	3.00	0.15	0.36	0.03	8.81	0.07	79.12	0.19	0.11	0.01	0.05	0.004	5.85	0.02	1.42	0.01	0.05	0.004
	831 surf pt3	TU19	18.48	0.94	0.42	0.02	2.53	0.04	65.46	0.18	0.62	0.02	0.94	0.01	0.78	0.01	8.17	0.03	0.07	0.01
	833 surf pt 1	TU21	17.70	0.90	0.28	0.03	2.13	0.05	64.40	0.22	0.44	0.03	1.21	0.02	0.43	0.01	10.32	0.04	0.08	0.01
	833 surf pt2	TU22	17.62	0.90	0.26	0.02	2.20	0.04	64.59	0.17	0.44	0.02	1.20	0.01	0.43	0.01	10.23	0.03	0.07	0.01
Thick blue fragments	832 surf pt 1	TU8	2.88	0.15	0.48	0.04	0.93	0.04	82.91	0.24	0.31	0.03	1.09	0.02	0.20	0.01	9.84	0.04	0.14	0.01
	832 surf pt 2	TU10	3.04	0.15	0.55	0.03	0.97	0.04	82.98	0.25	0.35	0.03	1.07	0.02	0.18	0.01	9.65	0.04	0.14	0.01
	832 surf pt 3	TU12	3.40	0.17	0.48	0.03	0.81	0.03	81.68	0.19	0.39	0.02	1.29	0.01	0.13	0.01	10.60	0.03	0.14	0.01
Fragile translucent fragments	834 surf pt 1	TU15	18.87	0.96	0.39	0.03	2.78	0.06	65.28	0.22	1.01	0.04	1.00	0.02	0.90	0.02	8.01	0.04	0.07	0.01
	834 surf pt 2	TU16	19.25	0.98	0.47	0.02	3.00	0.05	65.00	0.36	0.57	0.02	0.99	0.01	1.00	0.01	7.74	0.05	0.07	0.01

Code	MnO		Fe_2O_3		CoO		CuO		SrO		ZrO_2		CdO		SnO_2		Sb_2O_3		PbO		SUM
TU29	0.02	0.003	0.41	0.01	0.001	0.0005	0.051	0.001	0.069	0.001					0.27	0.07	2.41	0.04	0.02	0.02	99.99
TU30	0.02	0.002	0.51	0.01			0.008	0.0002	0.066	0.001	0.005	0.001			0.18	0.05	2.23	0.02	0.02	0.01	100.00
TU26	0.01	0.002	0.38	0.01	0.001	0.0003	0.018	0.0002	0.050	0.001	0.005	0.001	0.04	0.03			1.60	0.02	0.01	0.01	99.97
TU27	0.01	0.002	0.40	0.01			0.007	0.0001	0.054	0.001	0.006	0.001	0.13	0.03	0.26	0.06	1.86	0.02	0.01	0.01	99.99
TU28	0.01	0.002	0.38	0.01			0.008	0.0002	0.044	0.001			0.16	0.04	0.26	0.08	1.51	0.02			99.94
TU13	0.02	0.003	0.46	0.01	0.005	0.001	1.761	0.018	0.062	0.002	0.006	0.002	0.04	0.04	0.27	0.07	0.23	0.02	0.12	0.04	99.94
TU14	0.02	0.002	0.46	0.01	0.005	0.001	1.993	0.016	0.073	0.001	0.008	0.001			0.17	0.05	0.27	0.01	0.15	0.02	99.99
TU17			0.46	0.01	0.002	0.001	0.249	0.004	0.030	0.001	0.017	0.001	0.18	0.05			0.11	0.01			99.94
TU18			0.42	0.01	0.002	0.0005	0.257	0.003	0.038	0.001	0.021	0.001	0.17	0.03	0.15	0.06	0.15	0.01	0.01	0.01	100.00
TU19	0.01	0.002	0.39	0.01	0.002	0.0004	1.855	0.017	0.056	0.001							0.16	0.01			99.95
TU21	0.01	0.003	0.48	0.01	0.005	0.001	1.847	0.018	0.068	0.002	0.007	0.002			0.18	0.07	0.23	0.02	0.11	0.04	99.93
TU22	0.02	0.002	0.46	0.01	0.004	0.0005	1.813	0.015	0.068	0.001	0.008	0.001			0.23	0.05	0.25	0.01	0.11	0.02	100.00
TU8	0.01	0.003	0.37	0.01			0.003	0.0002	0.035	0.001	0.036	0.001			0.26	0.07	0.51	0.02			100.00
TU10	0.02	0.003	0.38	0.01			0.002	0.0002	0.036	0.001	0.038	0.001			0.15	0.06	0.45	0.02			100.00
TU12	0.01	0.002	0.35	0.01	0.001	0.0003	0.003	0.0001	0.040	0.001	0.040	0.001			0.05	0.05	0.54	0.01			99.96
TU15	0.02	0.003	0.33	0.01			0.002	0.0001	0.047	0.001			0.06	0.05	0.34	0.08	0.89	0.02			99.99
TU16	0.02	0.002	0.36	0.01	0.001	0.0003	0.003	0.0001	0.059	0.001	0.007	0.001	0.03	0.03	0.23	0.06	1.13	0.02	0.01	0.02	99.96

440 keV and the 1636 keV gamma rays produced by the $^{23}Na(p,p'\gamma)^{23}Na$ reaction, the latter superimposed to the 1634 keV gamma rays from the $^{23}Na(p, \alpha\gamma)^{20}Ne$. Gamma rays were collected by a cylindrical Lantanum Bromide (LaBr) detector (base 5 cm diameter and lenght 5 cm) located located at backward angle and at about 15 cm from the target. LaBr was preferred to a germanium detector (also in place) because it had a faster response time and superior efficiency (better statistics) while maintaining a good resolution for both the isolated 440 and 1634–1636 gamma peaks. Yields were translated to concentrations by comparison with standard reference glasses (NIST 621and NIST 1412) according to the equations:

$$C_Z = k \cdot C_Z^S \frac{N_\gamma}{N_\gamma^S} \frac{Q^S}{Q} S_G(E) = k \cdot S_s(E)$$

where C_z is the element Z concentration, N_γ is the gamma ray yield, Q is the collected charge (superscript S indicates the standard). $S_S(E)$, $S_G(E)$ are the specific energy loss of the proton in the standard and the archaeological glass. Below 500 keV the cross sections of the above cited nuclear reactions are low (IAEA Tecdoc-1822, 2017) and contribute very little to the yield. Energy loss curves of the two standards and a soda-lime glass of average composition (data from Oikonomou et al., 2018) were computed by the SRIM software package (Ziegler et al., 2008). From 500 keV onward, the three curves have a maximum difference from their average of 1.3% and an average difference of 0.8%. Therefore, we can assume $k = 1$ in the above equations. We first obtained the concentration versus yield/charge curve for the standards and fitted it with a linear function imposing zero intercept. The fitting function was then used to extract the Na_2O concentration of all the samples, including again the standards. With the Na_2O concentration fixed by PIGE, the PIXE concentrations of the other elements were renormalized for an overall concentration of 100%. The final result of the procedure is shown in Fig. 15 for the standards NIST 621 and NIST 1412. For elements above 1% in weight, the deviation from the certified values is at most a few percent. The results of the glass analysis are given in Table 2.

Table 2 shows that in a few cases the sodium concentration is much lower than we could expect from soda lime glasses produced in the 5th century BCE. We attribute that to an extension of the devitrification layer close or beyond the proton beam range in glass. Indeed one of the samples (SECYR 833) could be analysed on a cross section by Scanning Electron Microscopy coupled to Energy dispersive Spectrometry. As seen in Fig. 16, there is a clear morphological separation between the devitrified area (dark grey) and the glass bulk (clear area). This affects, as expected, the sample content of elemental Na that goes from 2.42 % in zone 833–3 to 6.30% in zone 833–4 to 22.89% in zone 833–5, which falls in the glass bulk.

Not only Na but also K could be lost by weathering, altering as well the PIXE calculated K_2O concentration; therefore affecting all other concentrations, due to their normalization at 100%. This is not the case for the glass samples that in Table 2 give $Na_2O > 4$. The Na and K oxide concentrations are in range with the sets of other data we are considering in our discussion (Fig. 17 left). Furthermore the oxide concentration given by SEM for the 833 sample glass core and for the same sample by our PIXE-PIGE method are coherent (Fig. 17 right).

A further view of our results is offered by a principal component analysis based on main and minor elements (standardized) of the base glass. The PCA (Fig. 18) shows that fragments from the three identified objects listed in Table1 are close in composition for each object. The two translucent bowls (SECYR 828 and 829), although similar in aspect,

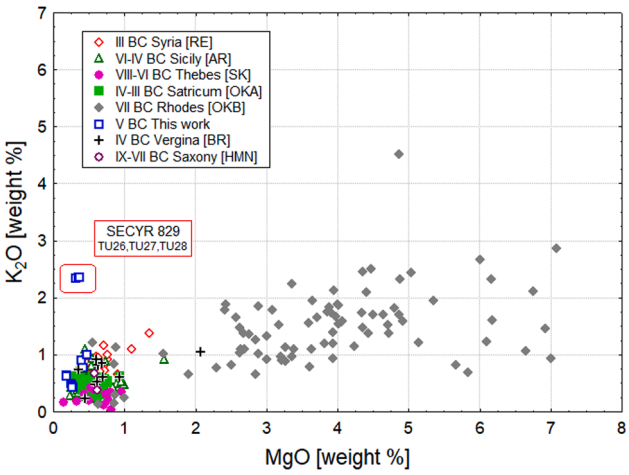


Fig. 19. The K_2O versus the MgO concentrations as measured in the Casas del Turuñuelo glasses. Comparison is made with data indicated by the following codes: RE (Reade and Privat, 2016), AR (Arletti, 2012), SK (Sokaras et al., 2009), OKA (Oikonomou et al., 2018), OKB (Oikonomou and Pavlos, 2018), BR (Brill and Lynus, 1994), HMN (Hartmann et al., 1997).

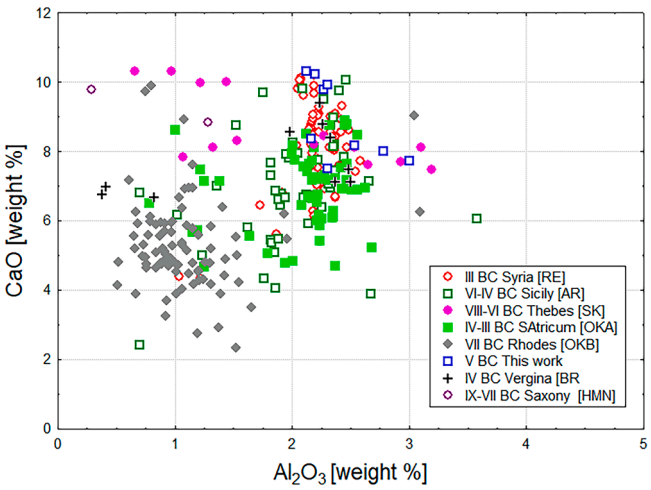


Fig. 20. The CaO versus the Al_2O_3 concentrations as measured in the Casas del Turuñuelo glasses. Comparison is made with data indicated by the same coding of Fig. 22. The samples TU26, 27, 28 are off scale in the X axis.

have a surprisingly different composition particularly in Al, K and Ca. The thin blue bowl (SECYR 830 and 833) has a base glass composition close to that of the bell-shaped bowl (SECYR 828). Sample SECYR 831 should in principle have been representative of the same thin blue bowl. Unfortunately only one measure (TU19) could be performed outside the remaining corrosion layer and that is instead close to the fragile translucent fragments (SECYR 834) from which it is distinguished by the content of the chromogens Cu and Sb. Since a few of the fragments received as SECYR 831 could not be reintegrated in the blue bowl it is well possible that the one taken for PIXE/PIGE analysis belonged to a different object. The samples having $Na_2O < 4$ are obviously well separated from all the other. Since the incresed concentration of potential fluxes (K, Pb) is well below the levels needed to form a glass, their anomalous compositions can be attributed to a persisting corroded surface layer.

The glass samples (Code TU) that in Table 2 give $Na_2O > 4$ have been used for comparison with the following published results on archaeological glasses:

(a) III century BC bowls (mainly) from the Hellenistic site of Jebel Khalid, Syria (Reade and Privat, 2016). Code RE.
(b) VI-IV century BC pre-Roman vessels and beads from Mozia (Sicily-Italy) (Arletti et al., 2012). Code AR.
(c) IV-II century BC Hellenistic glass vessels from Satricum (Italy) (Oikonomou et al., 2018). Code OKA.
(d) IX-VI century BC glass beads from Thebes (Greece) (Sokaras et al., 2009). Code SK.
(e) VII century BC archaic glass beads from Rhodes (Greece) (Oikonomou and Pavlos, 2018). Code OKB.
(f) VII-III century BC glasses from Greece of which five IV BC samples from Vergina (Brill and Lynus, 1994). Code BR.
(g) VIII-VI century BC glass fragments from Saxony (Hartmann et al., 1997). Code HMN.

4.1.1. *The glass bulk*

Considering all colours for the Casas del Turuñuelo and the literature samples, the bulk glass of Casas del Turuñuelo appears to be of the natron type. Also the glasses used for comparison (groups a) to g) above) are natron type with $10.42 < Na_2O < 23.5$. Indeed the majority of cases in Fig. 19 correspond to both K_2O and MgO below 1% in weight, as it is typical of the natron flux. Our translucent thick bowl (SECYR 829) has a K_2O concentration (TU26, 27, 28) around 2.3 % in weight which is higher than the other Turuñuelo glasses but with low MgO: values that remain outside the region expected for plant ashes. The use of mixed alkali cannot be ruled out for this specific glass which is also characterized by a relatively high Al_2O_3 content (see Table 2). It is to be noted that the 7th century BCE samples from Rhodes (Oikonomou and Pavlos, 2018) have MgO values higher than the rest of samples and can reach a maximum of 7.08%. Maybe Mg is brought into the composition by a calcium-source with dolomite impurities.

The peculiarity of the samples from Rhodes (Oikonomou and Pavlos, 2018) is evident also in the Al_2O_3-CaO bi-dimensional plot (Fig. 20) being both elements lower than for the other groups including Casas del Turuñuelo. As regards the sand component, for the Casas del Turuñuelo points we have calculated an average TiO_2/Fe_2O_3 ratio of 0.21 with a standard deviation of 0.09 derived from an Fe_2O_3 content lower than many of the compared samples but still compatible, within the errors, with what was found in more recent roman glasses (Zucchiatti et al., 2018).

4.1.2. *The colours of the Casas del Turuñuelo glasses*

No specific measurement (L*a*b, RGB, colour charts) has been done on the Turuñuelo samples. Some blue samples (TU8, TU10, TU12, TU17, TU18) have been measured in practice on the weathered layer and the quantification of possible chromophores in the bulk glass (some show Cu) is affected as explained above. As seen in Fig. 21, the chromatic agent was clearly identified as Cu for the other blue samples (TU13, TU14, TU19, TU21, TU22) that have $CuO = 1.86 \pm 0.09$ % (standard deviation). Only traces of cobalt are found. Copper has been identified as the colouring agent in turquoise vessels from Mozia (Arletti et al., 2012), in beads and pendants from the same site and in two alabastrons from Satricum (Oikonomou et al., 2018). Cobalt has been identified only in a bead from Mozia. A group of turquoise beads from Rhodes (Oikonomou and Pavlos, 2018) do not show the presence of copper.

The discolouring agent in the colourless glasses is antimony (see Fig. 21) which has the highest concentration in the bell-shaped translucent thick bowl (SECYR 828, measures TU29, TU30), a lower one in the translucent thick bowl (SECYR 829, measures TU26, TU27, TU28) and even lower in the fragile translucent fragments (SECYR 834 measures TU15, TU16). In Fig. 22 the comparison with samples from other works, listed above, shows that manganese is used only in samples of 3th century BCE (Reade and Privat, 2016). All earlier colourless samples we

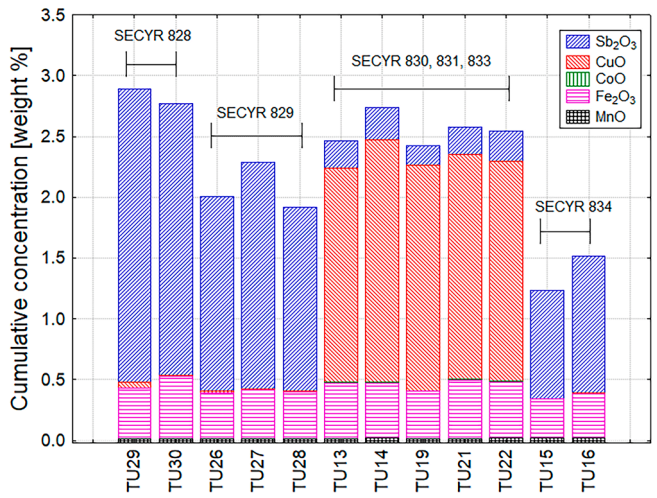


Fig. 21. The concentration of characterizing elements in glasses from Casas del Turuñuelo subdivided by their colour. See Table 2 for coding.

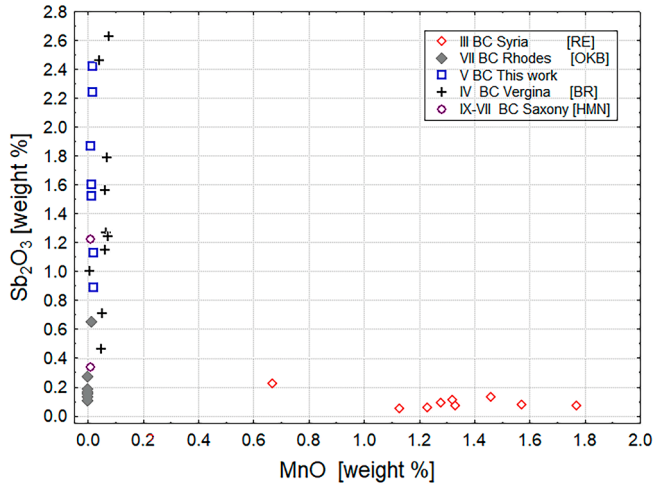


Fig. 22. The Sb_2O_3 versus the MnO concentrations as measured in the Casas del Turuñuelo colourless glasses. Comparison is made with data indicated by the same coding of Fig. 23.

considered are discoloured by antimony with the exception of a bead of the 7th century BCE (Oikonomou and Pavlos, 2018). It is worth noting that the Casas del Turuñuelo set covers the same range of concentrations as the set including the Vergina samples of 4th century BCE and five more samples from different sites in Greece dated from the 7th century BCE to 2th century BCE. The 7th century BCE samples from Rhodes (Oikonomou and Pavlos, 2018) have on average lower Sb_2O_3 concentration.

4.2. Isotope analysis and provenance

Two glass samples from Turuñuelo have been processed and analysed at the Laboratorio de Geocronología y Geoquímica Isotópica of the Universidad Complutense of Madrid. Strontium and neodymium isotopes have been quantified, following the same protocol used successfully in the characterisation of another set of glasses, also from a site in the Iberian Peninsula, but of Roman chronology (Zucchiatti et al., 2018).

These two elements have a very stable behaviour in most of the processes carried out over the glass production. Even at the relatively high temperatures of the glass melting process, no isotope fractionation takes place and the Sr and Nd signature of the glass will remain that of its raw materials. Therefore, differences in the Sr and/or Nd isotopic composition are a powerful tool for determining the origin of glass raw materials (Freestone et al., 2003; Gallo et al., 2015).

In Table 3 are summarized the results obtained for glass fragment 833 and 834 as well as control standards.

Weldeab and Coworkers (Weldeab et al., 2002b) have studied Mediterranean Sea sediments and demonstrated that the $^{87}Sr/^{88}Sr$ isotopic ratio goes roughly from its high at about 0.718 at 16°E (Sicily) down to about 0.709 at 35°E (Israel-Egypt) while εNd shows the opposite behaviour growing from its minimum of about −11.0 at 16°E to a high of about −2.0 at 35°E. It has to be noted that the dispersion of data is strongly influenced by the main pathways of riverine suspended matters in the Mediterranean Sea basin. All that considered the data obtained for the Casas del Turuñuelo glasses (Table 2) indicate that the material employed in the fabrication of our glasses should proceed from the Eastern Mediterranean area.

To find out more isotopic similarities we have compared the Casas del Turuñuelo data (Fig. 23) to the Sr and Nd isotopic analysis performed on: other natron glasses (Degryse and Schneider, 2008, Ganio et al., 2012, Blomme et al. 2016, Blomme et al 2017, Boschetti et al. 2017, Zucchiatti et al. 2018); natural sands from the Aegean (Blomme et al. 2016) as well as from sites in Belgium, Italy, Egypt and Israel, including the river Belus (Degryse and Schneider, 2008). Furthermore, surface sea sediments from the Eastern Mediterranean (Weldeab et al. 2002b) have been considered.

As already said, Casas del Turuñuelo fragments (Fig. 23 left) sit in the region of high εNd and low $^{87}Sr/^{88}Sr$ ratios i.e. the region corresponding to the Eastern Mediterranean, far away from the values shown by sediments in the Ionian and Sicily seas and also away from the sediments of the sea of Crete. Natron glasses dated from the 6th century BCE to the 5th century CE show an isotopic composition close to that of Casas del Turuñuelo glasses as concerns the $^{87}Sr/^{88}Sr$ ratio (see Table 4) but rather dispersed values of εNd. Their range is indicated by the dotted rectangle

Table 3
The results of isotopic analysis of samples SECYR 833 and 834.

Sample SECYR 833			**NBS 987**		**Jndi-1**	
87Sr/86Sr	**±StErr*10^{-6}**		**87Sr/86Sr**	**±StErr*10^{-6}**		
0.709410	3		*0.710243*	11		
143Nd/144Nd	**±StErr*10^{-6}**	**εNd**			**143Nd/144Nd**	**±StErr*10^{-6}**
0.512430	4	−4.1			0.512107	10
0.512387	1	−4.9				
			repetitions 10		repetitions 8	
Sample SECYR 834			**NBS 987**		**Jndi-1**	
87Sr/86Sr	**±StErr*10^{-6}**		**87Sr/86Sr**	**±StErr*10^{-6}**		
0.709271	*10*		*0.710241*	*14*		
143Nd/144Nd	**±StErr*10^{-6}**	**εNd**			**143Nd/144Nd**	**±StErr*10^{-6}**
0.512426	1	−4.14			0.512107	*5*
			repetitions 6		repetitions 5	

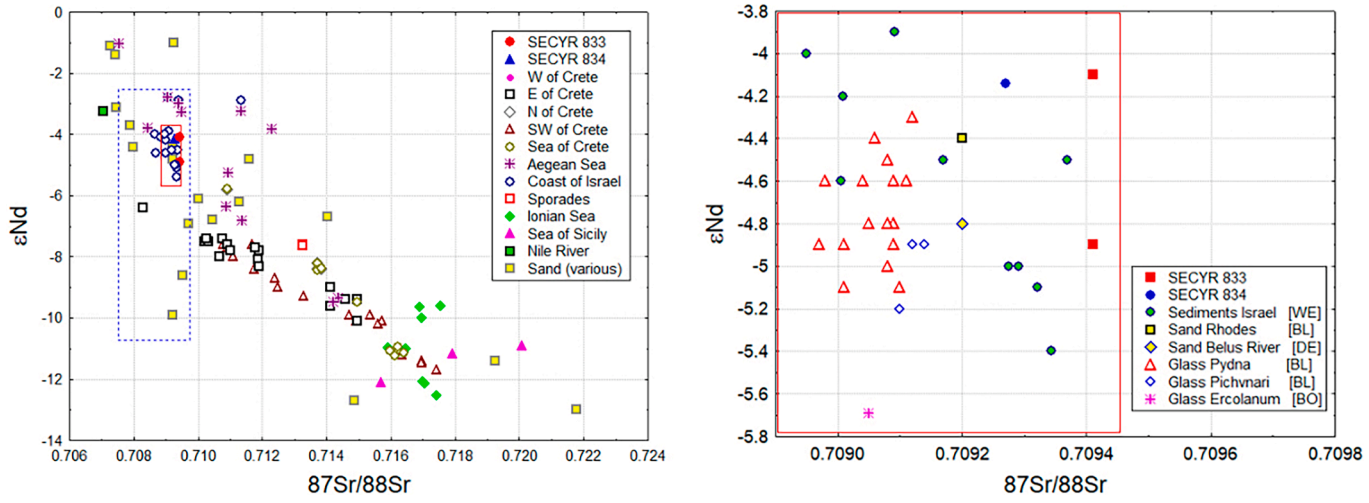


Fig. 23. The εNd versus the $^{87}Sr/^{88}Sr$ measured for the Casas del Turuñuelo samples SECYR 833 an SECYR 834. (left) Comparison with measurements on sands, marine sediments (see legend) and archaeological glasses of various provenances. Archaeological natron glasses dated from 8th century BCE to 1st century BCE are represented by the full line rectangle. Glasses dated from I AD onwards are represented by the dotted rectangle. (right) Expansion of the area indicated by the full line rectangle. See text for codes in legend.

Table 4
Statistics of the isotopic ratios and εNd for the ensemble of glasses taken into account (dotted rectangle in Fig. 23 left) and for the subset of glasses dated from 6th century BCE to 1st century BCE (full rectangle in Fig. 23 left and 23 right).

	$^{87}Sr/^{88}Sr$		$^{143}Nd/^{144}Nd$		εNd	
	All Glasses	VI BC-I BC	All Glasses	VI BC-I BC	All Glasses	VI BC-I BC
Valid cases	155	33	155	33	155	33
Mean	0.70901	0.70907	0.51236	0.51239	−5.41	−4.75
Minimum	0.70759	0.70875	0.51208	0.51234	−10.80	−5.69
Max	0.70966	0.70941	0.51251	0.51243	−2.50	−4.10
st.dev.	0.00022	0.00013	0.00007	0.00002	1.38	0.33

in Fig. 23 left. The region closer to our Casas del Turuñuelo results, marked by the full line rectangle in Fig. 23 left is expanded in Fig. 23 right. We observe proximity to the archaeological glasses of Pydna and Pichvnari (Blomme et al. 2016, Blomme et al. 2017. Code = BL) to sands from Rhodes (Blomme et al. 2017. Code = BL), sands from the Belus river (Degryse and Schneider, 2008. Code = DE) and marine sediments from Israel (Weldeab et al. 2002a. Code = WE). Isotopic analysis underlines that the nearest neighbours to the Casas del Turuñuelo glasses are natural specimen from the Eastern Mediterranean and glasses of the Hellenistic period.

5. Conclusions:

At the conclusion of the combined historical, conservation and analytical work we have achieved the main goals of this project.

The conservation protocol has managed to recover the shape and legibility of three glass bowls, allowing to implement their typological study and to establish parallels with objects from the Eastern Mediterranean.

Another objective was to implement typological and archaeological considerations on the objects with instrumental analyses aimed at identifying the glass types and possibly their origin. Combined PIXE-PIGE analyses have on one side put in evidence the persistence of some corrosion surface layer. On the other, have shown that the glasses are natron type fully compatible with Hellenistic production both for the base glass and the colouring/discolouring elements as detailed by comparison with several published data from the 9th to 3rd century BCE. In addition, isotopic analysis has located the production of Casas del Turuñuelo glasses in the Eastern Mediterranean and observed similarities with glasses from Pydna in the Macedonian area and from Picvnari a Greek settlement established on the Black Sea shore starting from middle 5th century BCE (Shortland and Schoerder 2009).

This connection is also detected from the typological analysis of the bowls. Based on the geographical dispersion of this type of production, we can determine the possible areas of origin of the same. These regions are Macedonia, Asia Minor and Rhodes. For the translucent bowls, we have examples from the Macedonian sites of Pydna, Derveni and Karitsa. However, locating parallels for the blue glass bowl is more difficult as it is not a common product. To date, it seems that we only have two parallels, corresponding to blue glass production, although one of them is quite distant from our object of study, both chronologically and technically. This is the bowl found in the Bernardini Tomb in Palestrina (Praeneste), from which a blue bowl dated to the first half of the 7th century BCE was recovered and which has been assigned a Syrian origin (Densmore Curtis, 1919). The second example, much closer to our specimen, is a bowl from a private collection now in the collection of the Corning Museum of Glass. Decorated with a 16-petal pointed rosette, its context is unknown, so it was dated by its Ephesian parallels to the 4th century BCE and is considered to be of Persian origin (Saldern, 1959:41).

Among the three vessels recovered, two typologies can be distinguished: on the one hand, two calyx-cups (Ignatiadou, 2013: 83), a group to which SECYR 828 and the blue bowl belong; while, on the other hand, the vessel with inventory number SECYR 829 belongs to the category of hemispherical skyphos (Ignatiadou, 2013: 113). The rest of the fragments, whose state of weathering does not allow their reintegration, cannot be identified at the typological level; however, from the incised decoration preserved on some fragments, we can consider that they must have belonged to a fourth, translucent bowl, similar to the two preserved ones.

Some authors have defended the possibility that these objects were not produced in the same places from which the raw materials are extracted and from which they were subsequently manufactured

(Ignatiadou, 2016). Although we will not enter into this debate, we are aware that the subject should be extensively reviewed in order to be able to delimit the areas of production. In this regard, we would only like to point out the scarcity of information available to locate the glass production workshops documented in the Eastern Mediterranean during the 1st Millennium BC, limited to the cases of Olympia, for the Classical period, and Rhodes (Ignatiadou, 2011: 72; 2016: 308–312).

Finally, we cannot fail to highlight the historical importance that the appearance of this batch of glass has for understanding the peninsular contexts of the 1st Millennium BC and, above all, the relations that existed at that time between the Eastern and Western Mediterranean.

As far as the sites in the interior of the Iberian Peninsula are concerned, specifically those located in the middle Guadiana valley, the imported objects documented to date were practically restricted to the appearance of Attic pottery. The presence of these products at sites dating from the 6th-4th centuries BC also coincides with the period when Athens held a monopoly on Mediterranean trade. (Domínguez Monedero and Sánchez Fernández, 2001). This explains the extensive collection of Attic goblets recovered in contexts of the Upper Guadiana (García Huertas et al., 2021) or at sites in the Middle Guadiana such as Cancho Roano (Gracia, 2003), to which we can now add the first examples recovered at the site of Casas del Turuñuelo (Celestino Pérez et al., 2017). To these are added the vitreous paste ointment jars, also present in the same context as the glass bowls analysed, and some imports of Etruscan origin (Celestino Pérez, 1991).

The appearance of these bowls demonstrates how the enclaves in the interior of the peninsula, between the 6th and 4th centuries BC, participated in Mediterranean trade networks. With their documentation, and together with the study of other materials such as Attic pottery, ivories or Pentelic marble sculpture, we can now analyse the trade routes and, what is almost even more important, try to identify which products or materials were used as currency for objects of the quality, beauty and luxury to which the batch of glass found in the courtyard of Casas del Turuñuelo belonged, to reach the interior of the peninsula.

Declaration of Competing Interest

The authors declare that they have no known competing financial interests or personal relationships that could have appeared to influence the work reported in this paper.

Data availability

No data was used for the research described in the article.

Acknowledgements:

This publication has been produced thanks to the support received from the State Research Agency of the Ministry of Science and Innovation, and is part of the R&D&I project: 'Building Tartessus 2.0. Constructive, spatial and territorial analysis of an architectural model in the middle valley of the Guadiana', PID2019-108180 GB-I00 (2020-2023), financed by MCIN/AEI/10.13039/501100011033. In addition, this research work has been carried out within the IJC2019-040888 financed by MCIN/AEI/10.13039/501100011033.

References

Arletti, R., Ferrari, D., Vezzalini, G., 2012. Pre-Roman glass from Mozia (Sicily-Italy): the first archaeometrical data. Journal of Archaeological Science 39, 3396–3401. https://doi.org/10.1016/j.jas.2012.06.009.

Blomme A., Degryse P., Dotsika E., Ignatiadou D., Longinelli A., Silvestri A. 2017. Provenance of polychrome and colourless 8the4th century BC glass from Pieria, Greece: A chemical and isotopic approach. *Journal of Archaeological Science*, 78, 134-146. http://dx.doi.org/10.1016%2Fj.jas.2016.12.003.

Blomme, A., Jan, E.J., Brems, D., Shortland, A., Dotsika, E., Degryse, P., 2016. Tracing the primary production location of core-formed glass vessels, Mediterranean Group. Journal of Archaeological Science Report 5, 1–9. https://doi.org/10.1016/j.jasrep.2015.10.031.

Boschetti, C., Julian, H.J., Jane, E.J., 2017. Mosaic tesserae from Italy and the production of Mediterranean coloured glass (4th century BCE–4th century CE). Part II: Isotopic provenance. Journal of Archaeological Science Report 11, 647–657. https://doi.org/10.1016/j.jasrep.2016.12.032.

Brill, R.H., Lynus Barnes, I.L., 1994. Laboratory Studies of Some Glasses from Vergina. The Journal of Glass Studies 36, 11–23.

Celestino Pérez, S., 1991. Cancho Roano, un complejo urbano orientalizante en Zalamea de la Serena (Badajoz). In: Remesal, J., Musso (coord.), O. (Eds.), La presencia de material etrusco en el ámbito de la colonización arcaica en la Península Ibérica. Barcelona, Universidad de Barcelona, pp. 439–456.

Celestino Pérez, S., Rodríguez González, E. 2019. Un espacio para el sacrificio: el patio del yacimiento tartésico de Casas del Turuñuelo (Guareña, Badajoz). *Complutum*, 30-2: 343-366. https://doi.org/10.5209/cmpl.66337.

Celestino Pérez, S., Rodríguez González, E. 2020. Actualidad en la investigación arqueológica en España: el yacimiento de Casas del Turuñuelo (Guareña, Badajoz), en A. Carretero y C. Papí (coord.), *Actualidad de la Investigación Arqueológica en España I (2018-2019)*. Museo Arqueológico Nacional, Madrid, 9-27.

Celestino Pérez, S., Gracia, F., Rodríguez González, E. 2017. "Copas para un banquete. La distribución de cerámicas áticas en Extremadura", in X. Aquilué, P. Cabrera and M. Orfila (coords.), *Homenaje a Glòria Trias Rubiés: cerámicas griegas de la Península Ibérica. Cincuenta años después (1967-2017)*. Barcelona, Centro Iberia Graeca, 140–149.

Celestino Pérez, S., López Ruiz, C., 2016. Tartessos and the phoenicians in Iberia. Oxford University Press, Oxford.

Climent-Font, A., Muñoz-Martin, A., Ynsa, M.D., Zucchiatti, A., 2008. Quantification of sodium in ancient roman glasses with ion beam analysis. *Nucluclear Instruments and Methods in Physics Research Section B: Beam Interaction with Materials and* Atoms 266, 640–648. https://doi.org/10.1016/j.nimb.2007.12.088.

Degryse, P., Schneider, J., 2008. Pliny the Elder and Sr and Nd isotopes: tracing the provenance of raw materials for Roman glass production. Journal of Archaeological Science 35, 1993–2000. https://doi.org/10.1016/j.jas.2008.01.002.

Densmore Curtis, C., 1919. The Bernardini Tomb. Memoirs of the American Academy in Rome 3, 9–90. https://doi.org/10.2307/4238513.

Dominguez Monedero, A., Sánchez Fernández, C., 2001. Greek pottery from the Iberian Peninsula. Brill, Leiden-Boston-Köln.

Freestone, I.C., Leslie, K.A., Thirlwall, M., Gorin-Rosen, Y., 2003. Strontium isotopes in the investigation of early glass production: Byzantine and early Islamic glass from the Near East. Archaeometry 45, 19–32. https://doi.org/10.1111/1475-4754.00094.

Gallo, F., Silvestri, A., Degryse, P., Ganio, M., Longinelli, A., Molin, G., 2015. Roman and late-Roman glass from North-eastern Italy: The isotopic perspective to provenance its raw materials. Journal of Archaeological Science 62, 55–65. https://doi.org/10.1016/j.jas.2015.07.004.

Ganio M., Boyen S., Fenn T., Scott R., Vanhoutte S., Domingo Gimenoc D., Degryse P., 2012. Roman glass across the Empire: an elemental and isotopic characterization. J. Anal. Atomic Spectrom., 27, 743-753. https://doi.org/10.1039/C2JA10355A.

García Huertas, R., Morales Hervás, F.J., Rodríguez González, D., Miguel-Naranjo, P., 2021. La huella helena en el Alto Guadiana a través de la presencia de cerámicas griegas. Abantos. Homenaje a Paloma Cabrera Bonet. Madrid, Ministerio de Cultura y Deporte, pp. 133–142.

Goldstein, S.M., 1979. Pre-Roman and Early Roman Glass in the Corning Museum of Glass. The Corning Museum of Glass, New York.

Gracia, F., 2003. Las cerámicas áticas del palacio-santuario de Cancho Roano. In: Celestino, S. (Ed.), Cancho Roano VIII: Los materiales arqueológicos I. Mérida, Junta de Extremadura, pp. 21–194.

Hartmann, G., Kappel, I., Gtote, K., Arndt, B., 1997. Chemistry and Technology of Prehistoric Glass from Lower Saxony and Hesse. Journal of Archaeological Science 24, 547–559. https://doi.org/10.1006/jasc.1996.0138.

IAEA TECDOC-1822 (2017) Development of a reference database for particle induced gamma ray emission (PIGE) spectroscopy.

Ignatiadou, D. 2011. "Υαλουργική τεχνολογία προρωμαϊκών χρόνων: ενιέα πλάνες περί την αρχαία υαλουργία", Ch. Gatxolis (ed). *AMTH Conservation Day 2009, GLASS*, 69-84.

Ignatiadou, D. 2013. *Coloursless glass for the élite in ancient Macedonia*. Υπουργείο Πολιτισμού και Αθλητισμού, Αρχαιολογικό Ινστιτούτο Μακεδονικών και Θρακικών Σπουδών. Δημοσιεύματα 13, Thessaloniki.

Ignatiadou, D. 2016. "Neither Phoenician nor Persian: glassworking in Archaic and Classical Greece", in F. Blondé (dir.), *LArtisanat en Grèce Ancienne: filières de production bilans methods et perspectives*. Villeneuve dAscq, Septentrion Presses Universitaires: 297-318.

Marín, B., Rodríguez González, E., Celestino Pérez, S., Gleba, M., 2019. Dressing the sacrifice: textiles, textile production and the sacrificial economy at Casas del Turuñuelo in fifth-century BC Iberia. Antiquity 93, 933–953. https://doi.org/10.15184/aqy.2019.42.

Newton, R., Davison, S., 1989. Conservation of Glass. Butterworths Series in Conservation and Museology, London.

Oikonomou, A., Pavlos T. 2018. An archaeometric study of Archaic glass from Rhodes, Greece: Technological and provenance issues, *Journal of Archaeological Science: Reports*, 22: 493–50. https://doi.org/10.1016/j.jasrep.2018.08.004.

Oikonomou, A., Henderson, J., Gnade, M., Chenery, S., Zacharias, N., 2018. An archaeometric study of Hellenistic glass vessels: evidence for multiple sources. Archaeological and Anthropological Science 10, 97–110. https://doi.org/10.1007/s12520-016-0336-x.

Palomar, T., Schibille, N., Rodríguez González, E., Celestino, S., Barrio, J., 2022. Shattered glass – An unusual alteration process in a 5th-century BCE archaeological

glass. In: ICOM-CC 22: Recent Advances in Glass and Ceramics Conservation 2022. ICOM, Lisbon, pp. 155–162.
Reade, J., Privat, K.L., 2016. Chemical characterisation of archaeological glasses from the Hellenistic site of Jebel Khalid, Syria by electron probe microanalysis. Heritage Science 4, 20. https://doi.org/10.1186/s40494-016-0084-3.
Rodríguez González, E., 2018. The Tartessian Tumuli of the Guadiana. Rivista di Studi Fenici 46, 117–136.
Rodríguez González, E., Celestino Pérez, S., 2017. Las estancias de los dioses: la habitación 100 del yacimiento de Casas del Turuñuelo (Guareña, Badajoz). Cuadernos de Prehistoria y Arqueología de la Universidad Autónoma de Madrid 43, 179–194. https://doi.org/10.15366/cupauam2017.43.006.
Rodríguez González, E., Celestino Pérez, S., 2019. Primeras evidencias de un banquete: análisis arquitectónico y material de la estancia S-1 del yacimiento de Casas del Turuñuelo (Guareña, Badajoz). Cuadernos de Prehistoria y Arqueología de la Universidad Autónoma de Madrid 45, 179–202. https://doi.org/10.15366/cupauam2019.45.006.
Rodríguez González, E., Celestino Pérez, S., Dorado-Alejos, A., Gutiérrez-Rodríguez, M. 2020. Stairway to Tartesós heaven: la escalera monumental del yacimiento de Casas del Turuñuelo (Guareña, Badajoz, España). Primeras evidencias de la fabricación de bloques con mortero de cal en la Península Ibérica, *Cuadernos de Prehistoria y Arqueología de la Universidad de Granada*, 30: 425-257. https://doi.org/10.30827/cpag.v30i0.15419.
Schmidt K. 2019. Glass and Glass Production in the Near East during the Iron Age. Evidence from objects, texts and chemical analysis. Oxford, Archaeopress.
Shortland, A.J., Schroeder, H., 2009. Analysis of first millennium BC glass vessels and beads from the Pichvnari necropolis, Georgia. Archaeometry 51, 947–965. https://doi.org/10.1111/j.1475-4754.2008.00443.x.
Sokaras, D., Karydas, A.G., Oikonomou, A., Zacharias, N., Beltsios, K., Kantarelou, V., 2009. Combined elemental analysis of ancient glass beads by means of ion beam, portable XRF, and EPMA techniques. Anal Bioanal Chem 395, 2199–2209. https://doi.org/10.1007/s00216-009-3156-3.
Vigil Pascual, M., 1969. El vidrio en el Mundo Antiguo. Instituto Español de Arqueología, CSIC, Madrid.
von Saldern, A., 1959. Glass finds at Gordion. Journal of Glass Studies 1, 22–49.
Weldeab S., Emeis K.C., Hemleben C., Vennemann T.W and Schulz H. 2002., Sr and Nd isotope composition of Late Pleistocene sapropels and nonsapropelic sediments from the Eastern Mediterranean Sea: Implications for detrital influx and climatic conditions in the source áreas, *Geochimica et Cosmochimica Acta*, 66: 3585–3598. https://doi.org/10.1016/S0016-7037(02)00954-7.
Weldeab, S., Emeis, K.C., Hemleben, C., Siebel, W., 2002b. Provenance of lithogenic surface sediments and pathways of riverine suspended matter in the Easter Mediterranean Sea: evidence from 143Nd/144Nd and 87Sr/86Sr ratios. Chem Geol 186, 139–149. https://doi.org/10.1016/S0009-2541(01)00415-6.
Ziegler, J., Biersack, J.P., Ziegler, M.D. 2008. Ion Straggle and TRIM: Output Files. In The Stopping and Range of Ions in Matter; Springer: Boston, MA, USA, 2008.
Zucchiatti, A., Climent-Font, A., Gutierrez Neira, P.C., Montero, R.I., Fuenlabrada, J.M., Galindo, C., 2018. Amorphous glass fragments from archaeological surface surveys: potential chronological use of ion beam and isotopic analytical characterization. Journal of Archaeological Science Report 19, 439–453. https://doi.org/10.1016/j.jasrep.2018.03.015.